applied sciences

MDPI

Article

Investigation of Inner Lining Loss and Correlation with Steel Structure Ovality in Rotary Kilns

David Zahradník *, Jakub Vynikal and Karel Pavelka

Department of Geomatic, Faculty of Civil Engineering, Czech Technical University in Prague, Thákurova 7, 166 36 Prague, Czech Republic; jakub.vynikal@fsv.cvut.cz (J.V.); karel.pavelka@fsv.cvut.cz (K.P.)
* Correspondence: david.zahradnik@fsv.cvut.cz

Abstract: The article delves into the application of laser scanning within the realm of engineering, concentrating its examination on rotary kilns. Through an in-depth case study, this article meticulously assesses the advantages inherent in utilising laser scanning technology and draws comparisons with conventional measurement methods. The overarching objective of the investigation is to unravel the intricate relationship between the deterioration of the rotary kiln liners and the ovality of the underlying steel structure. By meticulously analysing these aspects, this article seeks to contribute valuable insights into the understanding of this complex interplay in the context of engineering practices. As a measurement apparatus, a terrestrial laser scanner was used. The interior and exterior of the rotary kiln were measured. The primary focus object was inner-lining loss and the geometric characteristics of the cylindrical shells. The research uncovered significant disparities in inner lining loss between the sections. A correlation was found between the ovality and elimination of the inner lining. Due to the hypothesis of constant inner lining loss in the middle of the rotary kiln, the investigation found that the loss of brick lining was less than the value reported from the wells. This study offers significant information on the maintenance and repair strategies for rotary kilns, which have the potential to increase their efficiency and useful life.

Keywords: laser scanning; rotary kiln; geometry analysis

Citation: Zahradník, D.; Vynikal, J.; Pavelka, K. Investigation of Inner Lining Loss and Correlation with Steel Structure Ovality in Rotary Kilns. *Appl. Sci.* **2023**, *13*, 12811. https://doi.org/10.3390/app132312811

Academic Editors: Boštjan Kovačić, Rinaldo Paar and Ján Erdélyi

Received: 8 September 2023
Revised: 23 November 2023
Accepted: 24 November 2023
Published: 29 November 2023

1. Introduction

Laser scanning has become a common surveying technology over the past 30 years and is used for a variety of purposes. In engineering practice, it is used, for example, to determine volumes, measure deformations, and compare the state of an object over time based on a measured point cloud [1–3].

A rotary kiln is a large cylindrical industrial furnace that is used for drying, calcination, and chemical reactions, among other applications. Typically, it consists of a steel shell lined with refractory materials to withstand extreme temperatures [4–7]. Slowly and continuously rotating rotary kilns allow materials to be processed or heated as they move along the length of the kiln [8]. In industries such as cement production, lime production, and chemical processing, they are commonly used for clinker production, mineral roasting, and waste incineration. Figure 1 shows a measured rotary kiln with a terrestrial laser scanner.

A rotary kiln usually has a cylindrical shell, a riding ring, pads for the riding ring, thrust rollers, support rollers, and a method for turning the ring [9,10]. The scheme is shown in Figure 2 inside the shell. There is often a refractory lining that protects the shell from the high temperatures created by the operation of the kiln [11–16]. Depending on what the rotating kiln is used for, it may also have other parts, such as a cooler or a preheater.

Rotary kiln shape features

- Shape: the shape of the kiln as a whole, including any changes from a perfect cylinder.
- Size: the length and width of the kiln, as well as the depth.

- Symmetry: the degree to which the kiln is symmetric, including any differences from perfect symmetry.
- Wear and tear: the amount of wear and tear on the surface of the kiln, including any places where there is a lot of damage or wear.
- Ovality: the extent to which the cross-section of the kiln is circular or elliptical.
- Displacement: the amount that the kiln moves or shifts.
- Twist: the amount that the shaft of the kiln is turned.
- Deformations: any changes to the surface of the kiln.

Figure 1. Exterior of the rotary kiln.

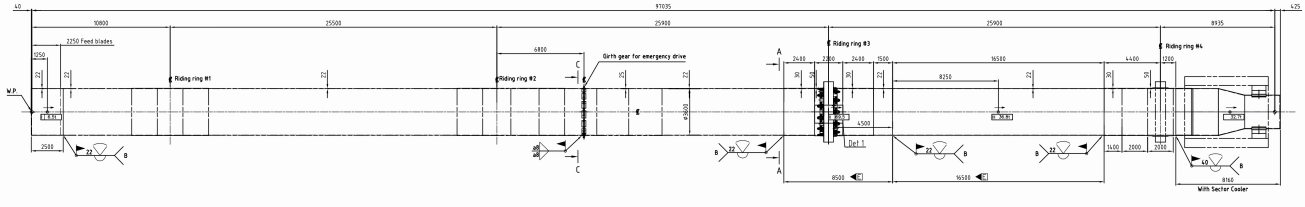

Figure 2. Rotary kiln scheme.

The cylindrical shell of a rotary kiln can be made of a number of different materials depending on what it will be used for and how it will be run. Carbon steel, stainless steel, refractory bricks, and cast refractory are all products that are often used. The focus is on the cylindrical shell of the rotary furnace and its geometric features such as the diameters of the parts that are welded together and how oval or round they are [17–22].

The deformation of the rotary kiln shell can cause a number of problems, such as the uneven wear of the refractory lining, bigger mechanical stress on the shell and support rollers, and a decline in the kiln's efficiency and ability to make things. Deformation can also cause the kiln to be out of place, which wastes energy and reduces the quality of the products. So, keeping an eye out and figuring out how the rotary kiln shell is changing is important to ensure that the kiln works well and lasts a long time [23].

Rotary kiln controls

- Checking the refractory lining for damage or wear that could cause the shell to overheat and change shape.
- Check for the wear or misalignment of the ring and support wheels, which can cause the shell to load and change shape.

- Check for wear or damage to the thrust rollers and thrust bearings, which can cause axial thrust loads that can cause the shell to bend.
- Making sure the drive system is aligned and working right, which can affect how the shell is loaded and where it is placed.
- Checking the shell for signs of cracks, deformation, or other damage, and fixing or replacing it as needed.
- Keep an eye on the kiln's temperature and other conditions and make changes as needed to prevent damage to the shell.

There are several ways to measure the ovality of a rotary oven. The shelltester is a tool used to measure how oval rotary kiln shells are. It does this by taking a picture of the drum's 3D surface profile, which gives a detailed picture of the drum's surface. It works with the help of a set of sensors that are placed around the kiln. At different points around the shell's diameter, the sensors measure how far away the shell is from the sensors. This enables the ovalness of the shell to be calculated [23–25].

High temperature around a total station, scanning the operating rotary kiln, affects the accuracy of the measurement. Refraction must be taken into account by using a thermal camera to measure the air temperature [26].

The total station can be used to determine how straight the shell's rotation axis is, where the bearing rollers and tyres are in relation to each other, and where their rotation axes are. When the rotating kiln is cold, it is possible to obtain better results [27].

One popular technique for measuring complex objects is laser scanning. Using laser scanning technology, a large number of 3D data points are collected, and then this information is used to make a detailed map of the building surface. It is possible to use point clouds to determine the displacement, curvature, spin, and so on [28].

Measuring with a terrestrial laser scanner (TLS) is faster than with a total station, but it takes longer to process the data. For further research, it is important to get rid of all (redundant points/data) [29]. By comparing two point clouds, it is possible to detect structural changes in time [30,31].

Some studies used the segmentation of raw point clouds to reduce the amount of time it took to process. The point cloud is broken up into different shapes, such as rotary rings, circular shells, and others. Geometric factors such as shape, size, symmetry, ovality, displacement, curvature, and twist can be estimated using segmented point clouds [29].

The laser tracker and high-precision total station is mostly used for rotary kiln drive alignment, which includes the position of the furnace axis, the centre-to-centre distance of the gears of the crown pair, radial and axial beats of the ring gear, etc. [31].

Another system made up of a laser system, a hall sensor, and a magnet is used to figure out the eccentricity of the radius, the deformation of the surface of the cylinder, and the eccentricity of the centre of the cross-section from the rotary kiln axis. The magnet and Hall sensor are placed on the meshing gear to make a pulse signal to start and stop laser data acquisition. Laser data are used to determine the coordinates of 3D points for further research [11].

After the annual lime firing process, the loss of the lining inside the rotary lime kiln was recorded. The people in charge of a rotary kiln have to check the loss every year and figure out where repairs need to be made. Each year, the readings of the wells show how much of the lining has been lost. The inner lining is drilled every two metres along the 42 m closest to the fire flame, which are the parts of the kiln that undergo the most wear. The drill bit is pushed through the brick until it hits the steel structure. The height of the rest of the inner cover is then decided. The loss can only be calculated at the point of drilling by comparing the ideal inner lining with the actual inner lining. Laser scanning is the best way to obtain information from the inside of a rotary kiln while limiting the number of useless cement points [32].

One of the most effective methods for thermal measurement in rotary kilns is infrared thermography. This non-contact, non-destructive technique uses infrared cameras to capture and analyse the thermal radiation emitted from the kiln surface. The resulting

thermal images provide valuable information on the temperature distribution and potential hotspots. [33] Hotspots can develop in rotary kilns due to a variety of factors, such as the uneven wear of the lining, blockages, or mechanical problems. Thermal imaging can be used to identify hotspots early, allowing for timely corrective action to prevent damage to the kiln or product quality issues. The quality of the product in the rotary kilns is highly dependent on the thermal profile. Thermal imaging can be used to ensure that the product is heated to the correct temperature and for the appropriate duration, resulting in a consistent and high quality product [34].

During a rotary kiln shutdown, point clouds were collected. Ladle refractory linings used in the steel industry can be checked for gaps and cracks with a special laser scanner [35].

We use the laser scanning method to determine how much of the inner layer has been lost. Every year, the internal lining of the rotary kiln is inspected and repaired as necessary. The inspection is performed by piercing the inner lining with a drill and then measuring the depth of the remaining brick. Unfortunately, since drilling is only performed in a single line along the entire length of the rotary kiln, measurements cannot be taken over the entire surface area of the rotary kiln. The laser scanner is used to measure the entire interior area and determine how much loss there is. There are different ways to determine the cost. The first option is based on the difference between the point cloud of the inner lining and the point cloud of the outer steel structure. To do this, the plans must show the thickness of the outer steel structure. The second choice is to make a perfect model of the inner lining and determine how different it is from the actual point cloud.

The previous work closest to this paper is Refractory Brick Lining Measurement and Monitoring in a Rotary Kiln with Terrestrial Laser Scanning [32]. Laser scanning with a Zoller + Fröhlich Imager® 5010c scanner of the interior of a rotary kiln was used to determine the loss of the interior lining. A cylinder was fit to the point cloud of the inner lining using the RANSAC [36] method and the CloudCompare software [37]. The cylinder axis was used to determine the rotation axis of the rotary kiln. In this paper, a similar method was chosen with the difference of determining the cylinder on the outer shell of the rotary kiln. On the steel outer shell, the deformations are not similar on the inner lining. The axis is determined on a better quality substrate without loading a large number of outliers.

The determination of the ovality of the rotary kiln by laser scanning has already been dealt with by [23,38,39]; this article does not deal with innovative solutions to improve the ovality results. The contribution of this article lies in finding the relationship between the loss of the inner lining and the ovality. At the same time, it lists the possible point cloud analysis if the rotary kiln is scanned inside and outside.

The correlation between lining loss and ovality in rotary kilns is a novel finding that has important implications for the maintenance and operation of these industrial vessels. Previous research has shown that lining loss is a major problem in rotary kilns, but the underlying causes of lining loss have not been fully understood. The new finding that ovality is a significant factor in lining loss provides a new avenue for research into the prevention and mitigation of lining loss. This paper introduces a laser scanning method that enables the simultaneous estimation of lining loss and ovality using a single measurement system. This innovative approach facilitates the examination and modelling of the correlation between lining loss and ovality. The laser scan data presented in this paper are applicable for additional analyses outlined in the study.

In the Material and Methods section, we elucidate the employed rotary kiln and its associated parameters. In addition, we detail the methods utilised for measurement and the procedural intricacies of the entire process. The Results section encompasses potential analyses derived from laser scan measurements, encompassing aspects such as the loss of inner lining, ovality, radius disparities, and the correlation between inner lining loss and ovality, along with the material loss in the riding ring. A noteworthy and innovative facet of the analysis lies in the utilisation of laser scanning to estimate the inner lining loss and

its correlation with ovality. The Discussion section outlines the limitations and conditions governing the application of the methods employed. In the Conclusions section, we provide a concise summary of the results and contemplate potential avenues for future research.

2. Materials and Methods

The measured object is a rotary lime kiln in the paper industry. The length of the kiln is 97 m, and the steel frame is 1.82 m in diameter. The kiln is about 3 m above the ground and is supported by four pedestals. There are two pedestals at each end of the furnace and two that are evenly spread along its length. On the two substations in the middle, there are motors that can be used to turn the furnace. The scheme is shown in Figure 2.

The burner itself is made of steel and has a lining inside. Most of the steel frame of the furnace is 22 mm thick, and the riding ring has reinforcements that are 30–50 mm thick.

The inner cover is split into several parts depending on the process being carried out: the burning zone, the intermediate zone, the heating zone, and the feeding zone (Figure 3). Most of the wear or loss occurs in the burning zone, where the high temperatures for lime firing break down the brick walls. Therefore, the inner lining becomes thicker in places where there is more wear than in other places. At the same time, the covering from the burning zone to the heating zone is made of two different materials to ensure adequate insulation.

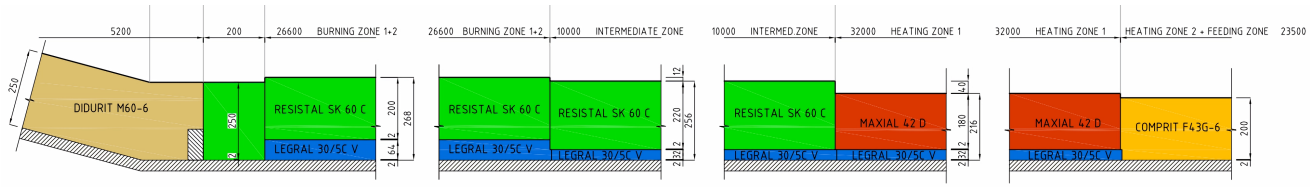

Figure 3. Detail of composition.

Methods used for monitoring rotary kilns

- Total station measurement: measuring the size of the kiln with an electronic surveying tool.
- Laser scanning: using laser scanners to take point cloud data of the kiln's surface and then processing the data to make a 3D model of the kiln.
- Terrestrial photogrammetry: A 3D model of the kiln is made from a collection of high-resolution photos taken from different angles.
- Infrared thermography: thermal imaging cameras are used to find areas of wear or damage on the surface of the oven where the temperature changes.
- Ultrasonic testing: the application of ultrasound sensors to measure the thickness of the kiln's shell and find places where it is getting thinner or eroding.
- Vibration analysis: using sensors to watch the kiln's vibration patterns and find any strange moves or vibrations that could hint at a possible problem.

A Leica RTC360 laser scanner (Leica Geosystems AG, Heinrich-Wild-Strasse, 9435 Heerbrugg, Switzerland) was used to measure the whole rotating kiln, as shown in Figure 4, The Leica RTC360 is a highly accurate laser scanning system used to capture the 3D measurements of objects, including rotary kilns. With a 3D point accuracy of up to ±2 mm, Ref. [40], it provides precise and reliable measurement results. The system's advanced laser scanning technology and intuitive software enable efficient data acquisition and analysis. It offers multiple scanning modes and incorporates positioning technology for accurate data registration. During the measurement, 86 laser scan positions were created. There were 19 spots created inside the rotary kiln, 31 positions created outside, and 36 positions constructed to connect the outside and interior of the rotary kiln. The outer shell had a scan resolution of 6 mm/10 m, and the inner shell had a resolution of 12 mm/10 m (Figure 5).

Figure 4. Leica RTC360 inside the rotary kiln.

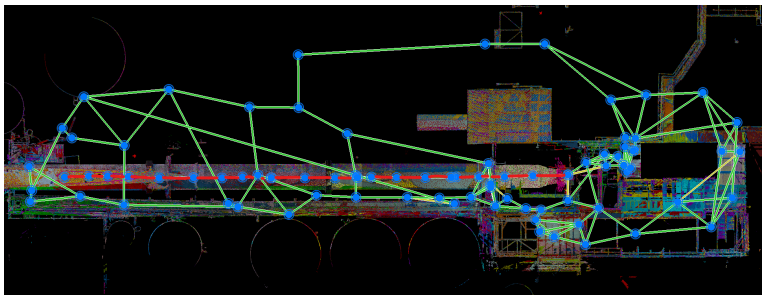

Figure 5. Scheme of laser scan's position (red—inner; green—outer).

Workflow

- Scanning rotary kiln exterior.
- Scanning rotary kiln interior with spherical targets.
- Scanning lime firing area to connect interior and exterior.
- Registration of scans in Leica Cyclone Register360.
- Clean scan from unnecessities.
- Export separately interior and exterior scans.
- Estimating axis of rotary kiln by fitting cylinder on exterior scans.
- Modelling perfect state of inner lining.
- Estimating lining loss by comparing model of perfect state with interior scans.

The steel frame on the outside and the brick walls on the inside were both measured. The connection between the interior and exterior was determined through the entrance of the kiln in the lime firing area. Two accessible spaces were used in the measurement to sufficiently register the interior. To maintain a large overlap for the cloud2cloud registration method, the maximum distance between the positions was 5 m. During readings, spherical targets were used to check and make sure that the registration was correct. Most of the time, the spherical targets were used to scan the inner lining to avoid misregistration, and the targets were spread out across the bottom of the rotating kiln in a way that was not symmetrical. During the scans, the kiln was not used and most of the lime was removed from the inside of the kiln. The rest of the lime was left on the bottom of the kiln, where it stuck strongly.

People and other unwanted things were removed from the point cloud that was left, leaving only the point cloud of the lime oven. The cloud was split into two datasets: an outer one that shows the steel frame and an inner one that shows the brick walls.

Two approaches were taken to calculate the lining loss. The first step was to determine the distance that separated the inner and outer cloud points. This distance determined the thickness of the entire structure of the pen, which encompassed the steel frame, the first and second layers of the brick lining, and the expansion that occurred between the layers. For this reason, it is essential to have a precise understanding of the thickness of the steel structure in order to calculate the lining loss. The expansion that occurs between the layers also has an effect on the final result.

The second approach requires a little more time and effort. To calculate the amount of loss, it is necessary to first construct a model based on the inner lining in its optimal state. This model will then be compared to the point cloud that represents the inner part. Because of this, it is necessary to identify the axis of the rotary kiln along which the ideal state model will be positioned in order to complete the process. The ambiguity on the abraded and deformed surface of the brick lining prevents the determination of the rotary kiln axis from being made using the point cloud of the inner lining. This is because the rotary kiln was built with bricks. The axes can be determined on the outer steel structure. For the rotary kiln to function as it should, the steel structure must be manufactured with a high degree of precision to ensure circularity and symmetry. The axis of the rotary kiln was located by employing the RANSAC method for detecting primitive objects within the point cloud that is part of the CloudCompare software. The radius range of the cylinder was defined to be 1.82 m ± 2 cm, so it would be easier to detect. The axis of this structure corresponds to the axis of the rotary kiln. A model of the ideal condition was modelled according to the determined axis and knowledge of the radius of the kiln interior from the composition of the brick lining to determine the loss of the inner lining. This was achieved by modelling a model of the ideal condition. The lining loss was calculated by comparing the ideal model to the measured point cloud of the rotary kiln's interior. This allowed the identification of the lining loss.

2.1. RANSAC Algorithm

The RANSAC algorithm is an iterative method used to estimate the parameters of a mathematical model from a set of observed data that contain outliers, when outliers do not have influence on the values of the estimates. It is a non-deterministic algorithm that uses repeated random subsampling and voting to find the optimal fitting result. The algorithm was first published by Fischler and Bolles at SRI International in 1981 [41].

Random Sample Selection:	$D_{\text{subset}} = \{(x_i, y_i)\}_{i=1}^{k}$
Model Estimation:	$\text{Model} = \text{Estimate Model}(D_{\text{subset}})$
Inlier classification:	$\text{Inliers} = \{(x_i, y_i) \mid \text{Error}(x_i, y_i, \text{Model}) < \text{Tolerance}\}$
Repeat:	(Repeat steps 1–3)
Best Model Selection:	$\text{Best Model} = \text{Model with Maximum Inliers}$

2.2. Laser Scanner Working Principles

Time of Flight Calculation:	$t = \frac{T}{2}$
Distance Calculation:	$R = \frac{ct}{2}$

The data that were collected can be used to estimate other physical features of the rotary kiln for further analysis:

- Rotary kiln ovality analysis.
- Radius difference along rotary kiln.

- Centrality of rotary kiln steel strip.
- Material loss of riding rings.
- Correlation of inner lining loss and ovality.

3. Results

3.1. Loss of Inner Lining

The loss of the interior lining was determined by measuring the difference between the ideal undamaged condition and the actual measured condition using a laser scanner. The initial hypothesis was that the interior lining of the perpendicular section of the rotary kiln wore evenly. Greater wear occurs close to the flame, whereas the risk of wear decreases with distance. Most of the lime has been removed from the interior of the kiln. Unfortunately, it was not possible to remove all the residue, so the lime remains on the bottom of the kiln and in areas where it has adhered. To obtain optimal results for comparing the laser scanning procedure with boreholes, the loss was statistically determined within a perpendicular section. By stationing, the rotary kiln was divided into dozens of 1-metre sections. The median values of the declines in a given section were used to define the decline from the difference model. The section's utmost value defined the loss in the joint between the bricks. On the other hand, the minimum value consisted of contaminated lime (Figure 6).

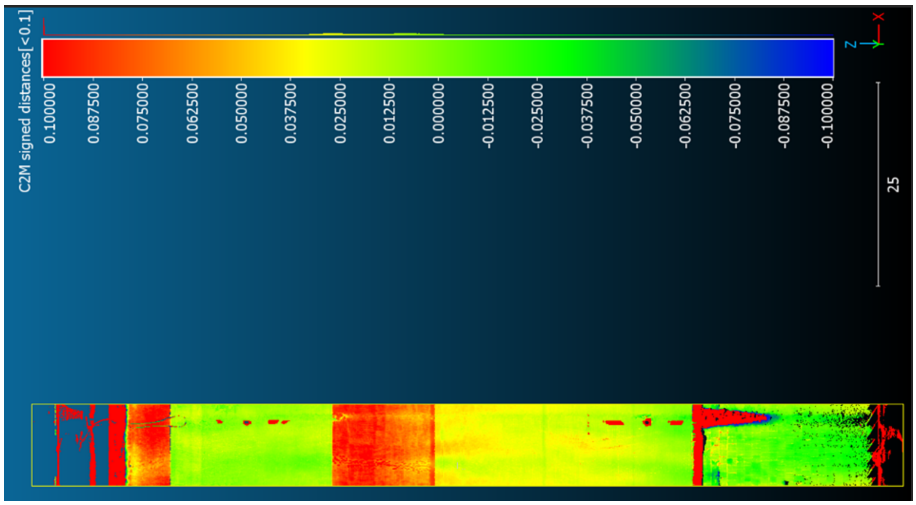

Figure 6. Inner lining loss inside the rotary kiln.

When the difference model and the measured numbers from the wells were compared, they were about the same. It was found that, after 42 m of stationing, the managers stopped measuring the loss of the liner and just assumed that the liners were always worn out. However, it was found that the loss of brick covering was less than that reported from the wells (Figures 7 and 8). Due to not cleaning the lime off the bricks well enough, the median loss went from 6 metres to 66 metres of staging. Most of the brick lining in the part from 66 metres to stopping was made of lime. At the same time, it was not expected that the brick lining would show much wear along this length. Due to the high frequency of lime in the brick lining, it was not further examined from 74 m from the stationing.

The original idea that there was constant wear in the vertical part of the furnace was also shown to be wrong. Between 42 and 46 m of rotary kiln length, there were large differences in the inner loss. At the brick joint, the loss was up to 52 mm. At the brick face, it was 35 mm, and at another spot, it was 12 mm. The big difference could be because the steel frame is oval-shaped (Figure 9).

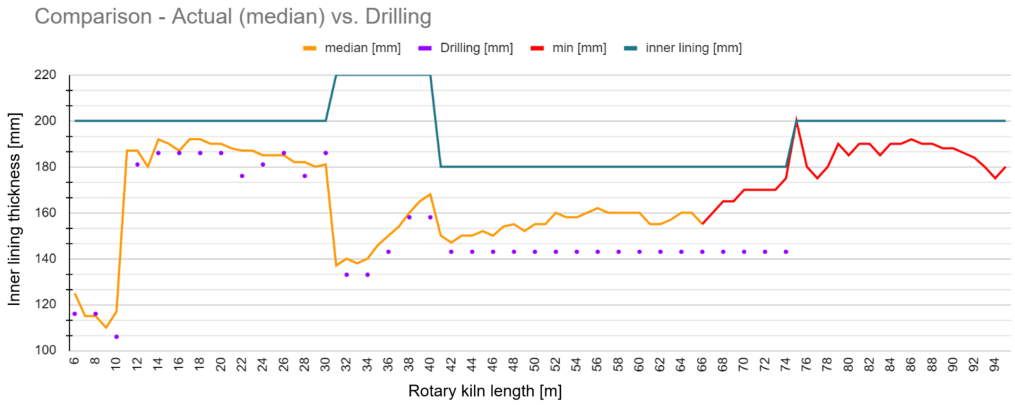

Figure 7. Comparison of the lining loss by laser scanning and drilling with ideal conditions (purple dots, drilling, orange, median loss from scanning, red, min loss from scanning, teal, ideal state of inner lining).

Figure 8. Comparison of maximum, median, min values of lining loss by laser scanning (min—red; orange—median; green—max; teal—ideal state of inner lining).

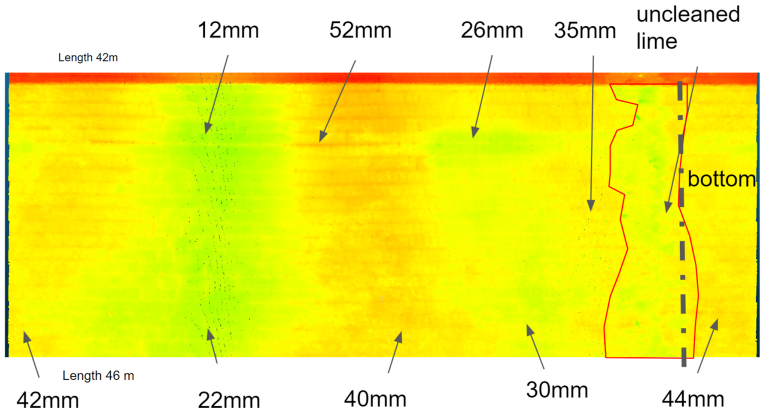

Figure 9. Wear differences in the 42–46 m perpendicular section of the rotary kiln.

3.2. Ovality

Using a reference cylinder model, the ovality was determined. Using the RANSAC method for detecting primordial objects from the point cloud, the cylinder was determined. Before detection, the cloud was removed to remove impediments to accurate measurement. For the purpose of detection, the radius of the potential cylinder was restricted to between

1.80 and 1.84 m. Derived from the difference between the detected cylinder and the measured point cloud, the resulting ovality was moulded (Figure 10).

This rotating kiln can be a −2 cm or +2 cm oval. The ovality was ploughed outside of the rotating rings (Figure 11).

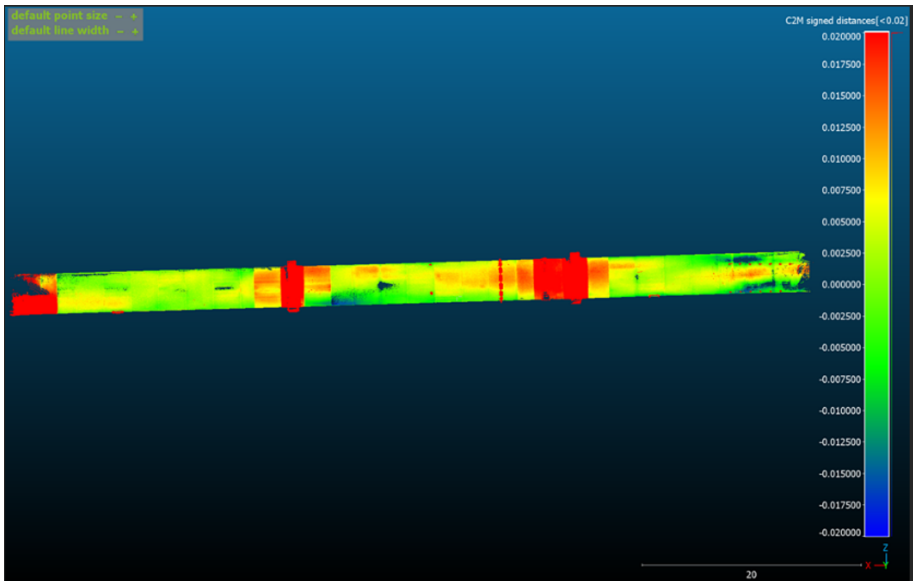

Figure 10. Rotary kiln ovality 3D (m).

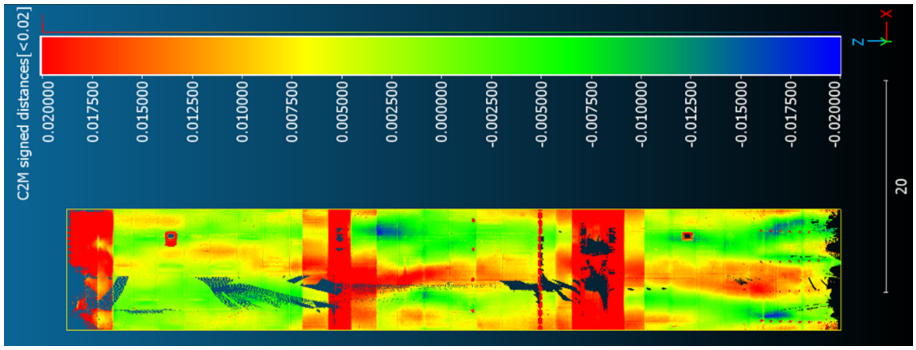

Figure 11. Rotary kiln ovality 2D (m).

3.3. Radius Difference

To determine the changes in radius and centricity, the steel structure cloud was divided by the welded webs (Figure 12). There are 29 steel strips of different lengths. The RANSAC method was used to find the cylinders in each strip over a radius range of 1.80–1.84 m. On average, the difference from the drawing radius was found to be 5 mm (Figure 13). The biggest changes were found in the webs around the riding ring. Even in the drawings the steel structure is getting thicker. The position of the centre of the cylinder is extracted from the detected cylinders of each steel strip. Using the least squares method, the rotary kiln axis was found by taking the values found. To determine the centricity, the difference between each steel strip and the axis of the rotating kiln was used. The largest amount of irregularity was 18 mm (Figure 14).

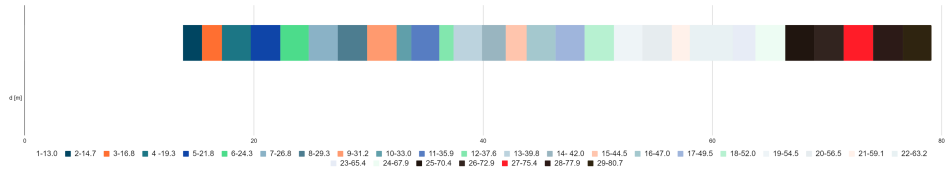

Figure 12. Rotary kiln steel strips scheme (m).

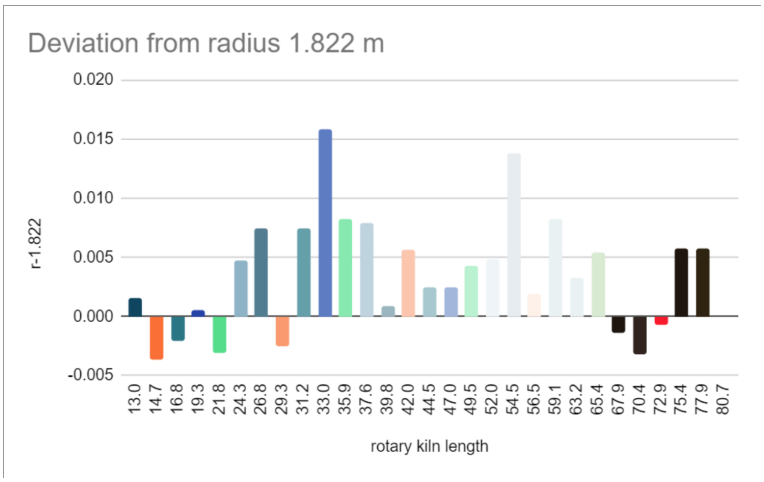

Figure 13. Difference in the radius of steel strips (m).

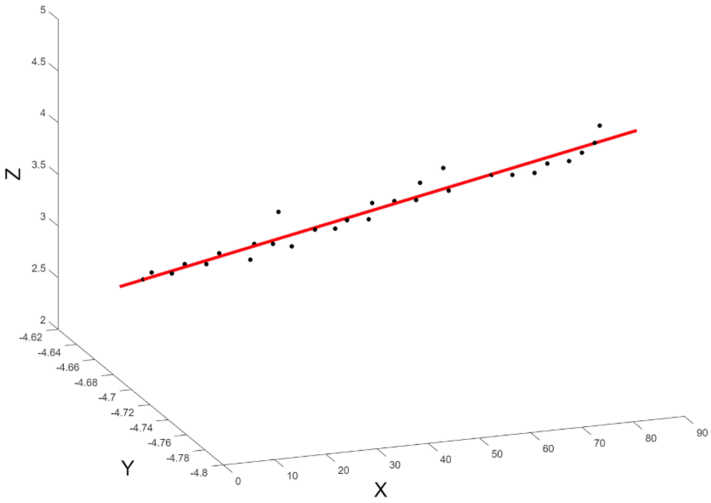

Figure 14. Steel strip centricity (m).

3.4. Correlation of Inner Lining Loss and Ovality

The expanded cylinders of the plane in the raster were the source of the data used in the process to establish whether or not there was a correlation between the loss of internal lining and the ovality of the steel structure. The values of raster ovality ranged from −5 cm to +5 cm in either direction. It was revealed that the figures for the loss of internal lining could range anywhere from ten centimetres in either direction. Due to the resolution of the difference model, neither of the rasters was free from the presence of null data. A point cloud constitutes the difference model, and each individual point stores a value corresponding to the difference.(Figure 15)

In order to analyse the correlation, a grid of 2 cm squares and 2.1 million points was developed. Each point received a value determined by the grid to which it was part. Following that, a filtering of the points needed to be carried out on the null data as well as

for the points that had maximum values of ovality and inner lining loss. The total number of points is now 270,000 less than before.(Figure 16)

$$\rho = \frac{\sum_{i=1}^{n}(x_i - \bar{x})(y_i - \bar{y})}{\sqrt{\sum_{i=1}^{n}(x_i - \bar{x})^2} \cdot \sqrt{\sum_{i=1}^{n}(y_i - \bar{y})^2}} \quad (1)$$

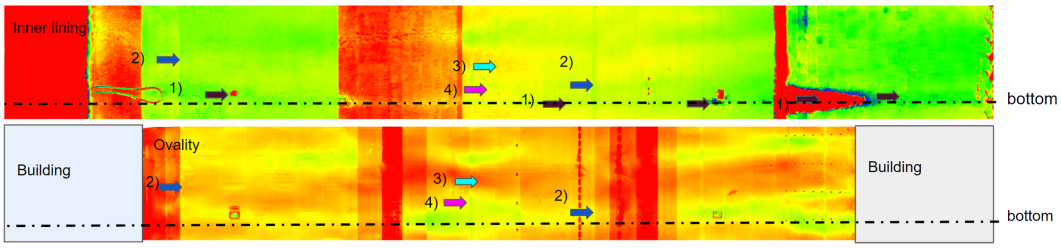

Figure 15. Lining loss—upper; ovality—lower: (1) lime that has not been cleaned; (2) corresponding welds with small lining loss; (3) positive ovality means more lining loss; and (4) negative ovality means less lining loss.

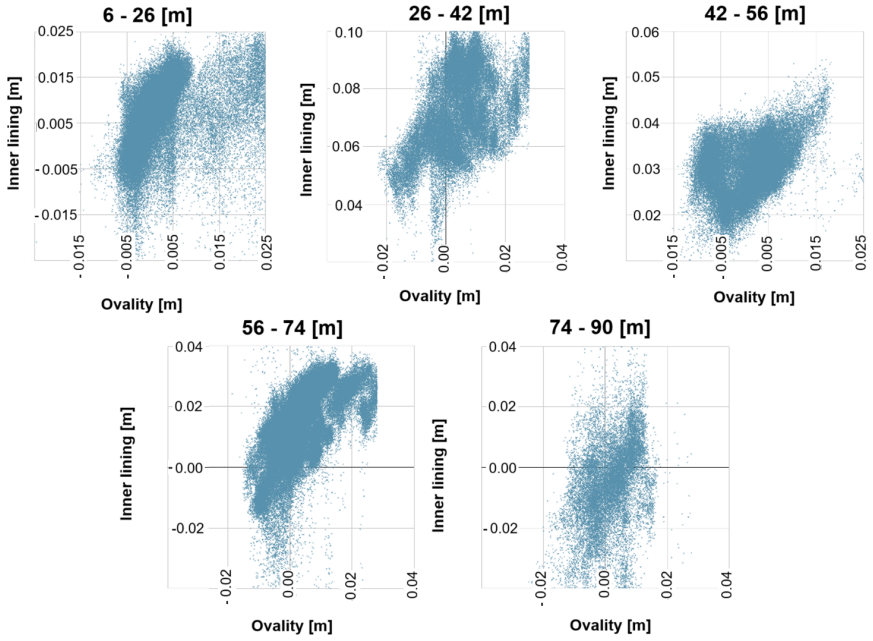

Figure 16. Correlation ovality and rotary kiln: 0–26 m; 26–42 m; 42–56 m; 56–74 m; and 74–90 m.

3.5. Riding Ring Materials Loss

It is feasible to establish the level of wear that the riding rings have sustained based on the measured data. The precision of the scanner [40] and the degree to which the shining surface of the ring of the rider reflects light play a significant role in determining the outcome. The point cloud was attached to a part that only contained the riding rings in order to perform wear detection on the component. In the clipped sling, RANSAC cylinder detection was attempted, but regrettably, this method was insufficient due to the low height of the discovered cylinder. The search method was unable to correctly establish the location on the point cloud of the cylinder's axis, as well as its position. The most significant inaccuracy occurred during the process of determining the cylinder axis, which ultimately turned out to be a systematic variation in the difference model.

Blender software was used to perform a procedure that involved the manual alignment of a cylinder with a radius of 4.700 m. The rotation axis of the kiln drum was known from ovality analysis, the axis was also used as the riding ring axis. The cylinder with a radius of 4.700 m was created in Blender software and adapted to the rotation axis. The cylindrical

was moved along the axis to the position of the riding ring point cloud. Manual alignment produced superior results compared to the automatic detection strategy. On the riding rings, there was no evidence of any major systematic loss. The size of the riding ring is 3 millimetres larger than what is shown in the drawings. The values derived from the difference model have a normal distribution, since the variance and the mean error are 1 mm (Figure 17).

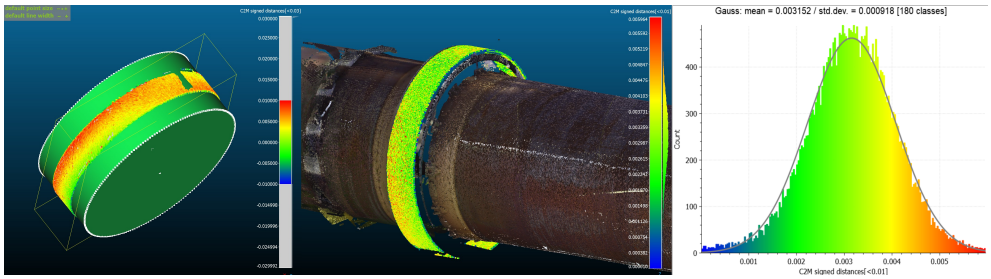

Figure 17. Imperfect RANSAC cylinder detection (**left**), manual alignment of ideal cylinder (**middle**), and distribution of the values of riding ring loss (**right**).

4. Discussion

This article provides an evaluation of two methods, namely laser scanning and drilling, to estimate the loss of lining in rotary kilns. Laser scanning offers several advantages as a non-destructive technique. It enables comprehensive data acquisition, capturing the detailed geometry of the kiln's inner surface, and facilitating precise measurements. Laser scanning is time-efficient, requires minimal setup, and eliminates the need for physical contact with the kiln, reducing safety risks. However, it has limitations, including high costs for equipment and data processing, limited penetration depth, and susceptibility to environmental conditions such as high temperatures and pollution.

However, drilling provides direct measurements of the thickness of the lining, making it a reliable method of estimating loss. It is a cost-effective approach that utilises basic equipment and techniques. However, drilling is a destructive method that may cause structural damage and provide limited samples, potentially underestimating the extent of the lining loss.The choice between laser scanning and drilling depends on various factors, such as project requirements, precision needed, the magnitude of lining loss, costs, schedule constraints, and kiln condition. A thorough analysis of these factors can determine the optimal method for estimating the loss of insulation in a rotary kiln (Table 1).

Table 1. Comparison—drilling versus terrestrial laser scanning.

Subject	Drilling	TLS
Measurement time	2 h	5 h
Processing time	0 h	3 h
Cover area	1%	95%
3D visualisation	no	yes
Exact periodic comparison	no	yes
Gap detection	no	yes

Furthermore, this study investigated the relationship between inner lining loss and the design of the kiln steel frame. The findings revealed a positive correlation, indicating that higher ovality values were associated with greater lining loss. This highlights the importance of considering structural changes when assessing the integrity of the kiln's inner layer. The correlation coefficients ranging from 0.38 to 0.57 indicate a moderate to moderately strong positive correlation between the ovality and lining loss in the studied rotary kiln. Although these coefficients may not be exceptionally high, they signify a significant relationship between the variables (Table 2).

This study also discovered that the loss of brick lining is less than the value reported from the wells. The resulting median loss was taken from 6 metres to 66 m of the stope due to inadequate lime brick lining cleaning, which occupied most of the brick lining area in the section that began at 66 m of the stope. At the same time, it was no longer anticipated that the brick lining throughout this length would show significant wear. Due to the high frequency of lime in the brick lining, the marquee could not be viewed much further from its 74 m vantage point (Figure 7).

Table 2. Pearson correlation coefficient estimated on parts of rotary kiln.

Length of Rotary Kiln	Pearson Correlation Coefficient
6–26 m	0.38
26–42 m	0.47
42–56 m	0.57
56–74 m	0.36
74–90 m	0.44

The method of estimation of lining loss in rotary kiln with laser scanning is simple to apply on any rotary kiln. The main factors to use laser scanning for the analysis of the rotary kiln are the visibility of the rotary kiln itself. If the rotary kiln is surrounded by other technology and a large part of it is not visible, the following analysis steps cannot be performed. A follow-up condition is sufficient space to connect scans inside and outside the rotary kiln. Smaller and narrower interconnection spaces will impair the quality of point cloud from laser scans. A similar condition of visibility applies inside the rotary kiln. Material must be visible for the analysis of loss of internal lining. If the masonry is contaminated with lime or other material, the scanner is unable to measure the condition of the internal lining.

5. Conclusions

The purpose of the research was to establish a relation to the ovality of the steel structure and the amount of material that was lost from the inside lining of the rotary kiln. It was determined how much of the inner lining had been lost by making a comparison between the ideal condition (one in which there was no damage) and the real condition (one that was measured using a laser scanner). According to the results of the research, the prediction that the perpendicular part of the furnace would experience consistent wear was erroneous. The investigation indicated that there were considerable variances in the amount of loss detected between sections. The joint noticed the greatest loss, which measured up to 52 mm, while the face of the bricks experienced a loss of 35 mm and 12 mm elsewhere. The ovality of the rotating kiln ranged from minus two centimetres to plus two centimetres and was measured outside the rotary rings. The location of the centre of the cylinder was derived from the observed cylinders of each steel strip, and the axis of the rotary kiln was located using a method that minimised the sum of the squared deviations. The eccentricity reached a peak value of 18 mm at its highest point.

The ovality of the steel structure was measured using a 2 cm grid containing 2.1 million points. Each point was given a value from this grid so that the correlation between the loss of internal lining and the ovality of the steel structure could be determined. Filtering out null data and points with maximum ovality values and the loss of internal lining led to a reduction in the total number of points, which was reduced to 270,000. According to the study findings, there is a significant link between ovality and lining loss, with Pearson's correlation coefficients ranging anywhere from 0.38 to 0.57 depending on the portion of the furnace analysed. The preciseness of the scanner as well as the reflectivity of the smooth shining surface of the slider ring both have a significant impact on the final output.

In summary, the research reveals important information on the internal lining loss of the rotary kiln and the correlation between this loss and the ovality of the steel structure. This study demonstrates both the importance of properly cleaning the brick lining from

lime to produce accurate measurements and the limits of the laser scanner in identifying wear on the shining surface of the travelling ring. Both of these issues are highlighted in the study. The results of the study have the potential to be used as a foundation for developing maintenance and repair techniques for rotary kilns, which can ultimately result in greater productivity and longevity.

Future work will focus on the evaluation method of period measurement. Each year, the rotary kiln will be measured and the actual results will be compared with previous results. Changes in ovality and lining loss will be monitored and examined with current results. Thermometers also monitor the rotary kiln of this paper, providing real-time insights into the distribution of heat and potential hotspots. Thermal measurement will be added to analyses of the correlation of ovality and lining loss.

Author Contributions: Conceptualisation, D.Z.; methodology, D.Z.; validation, D.Z. and J.V.; formal analysis, D.Z.; investigation, J.V.; resources, D.Z.; data curation, D.Z.; writing—original draft preparation, D.Z.; writing—review and editing, D.Z.; visualisation, K.P.; supervision, K.P.; project administration, K.P.; funding acquisition, K.P. All authors have read and agreed to the published version of the manuscript.

Funding: This work was supported by the grants SGS23/052/OHK1/1T/11 and SGS23/050/OHK1/1T/11 funded by CTU Prague, Czech Republic.

Institutional Review Board Statement: Not applicable.

Informed Consent Statement: Not applicable.

Data Availability Statement: The data is not available to protect the privacy of the plant that owns the rotary kiln.

Acknowledgments: Many thanks to the reviewers and the editor for their useful comments and suggestions.

Conflicts of Interest: The authors declare no conflict of interest.

Abbreviations

The following abbreviations are used in this manuscript:

RANSAC	Random sample consensus
TLS	Terrestrial laser scanning

References

1. Feber, N.; Jandera, M.; Křemen, T.; Rossi, B. Experimental study of welded austenitic stainless steel I-section beam-columns. In Proceedings of the EUROSTEEL 2021 Sheffield—Steel's Coming Home, Sheffield, UK, 1–3 September 2021; Ernst Sohn: Berlin, Germany, 2021; Volume 4, pp. 2255–2261. ISSN 2509-7075.
2. Mára, M.; Máca, P.; Sovják, R.; Šedina, J.; Curbach, M. The influence of various loading rates on concrete fracture surface areas. *Mater. Today Proc.* **2020**, *32*, 219–223. ISSN 2214-7853. [CrossRef]
3. Pavelka, K.; Šedina, J. Use of photogrammetrical methods and laser scanning for documentation of deformation at sequential loading. In Proceedings of the International Conference on Engineering Sciences and Technologies, High Tatras, Slovakia, 27–29 May 2015. ISBN 978-80-553-2042-7.
4. Xiao, Y.; Li, X.; Chen, X. General solution to kiln support reactions and multi-objective fuzzy optimization of kiln axis alignment. *Struct. Multidiscip. Optim.* **2008**, *36*, 319–327. [CrossRef]
5. Dhillon, B.S. Multiaxial fatigue life prediction of kiln roller under axis line deflection. *Appl. Math. Mech.* **2010**, *31*, 205–214. [CrossRef]
6. Pazand, K.; Panahi, M.S.; Pourabdoli, M. Simulating the mechanical behavior of a rotary cement kiln using artificial neural networks. *Mater. Des.* **2009**, *30*, 3468–3473. [CrossRef]
7. Ramanenka, D.; Stjernberg, J.; Jonsén, P. FEM investigation of global mechanisms affecting brick lining stability in a rotary kiln in cold state. *Eng. Fail. Anal.* **2016**, *59*, 554–569. [CrossRef]
8. Peray, W. *The Rotary Cement Kiln*; Edward Arnold: New York, NY, USA, 1986; pp. 227–343.
9. Ozek Makina. Available online: http://www.rotarykiln.net (accessed on 6 October 2020).
10. NAK Kiln Services. Available online: https://nak-kiln.com (accessed on 6 October 2020).

11. Zheng, K.; Zhang, Y.; Liu, L.; Zhao, C. Metoda računalnog mjerenja odstupanja ravnosti cilindra rotacijske peći. *Teh. Vjesn.* **2017**, *24*, 1297–1305. [CrossRef]
12. Rusinski, E.; Stamboliska, Z.; Moczko, P. Proactive control system of condition of low-speed cement machinery. *Autom. Constr.* **2013**, *31*, 313–324. [CrossRef]
13. Rahman, M.M.; Nijemeisland, M.; Wesselink, R.J.; Luding, S. Coupled CFD-DEM simulation of heat transfer and particle motion in a rotary kiln. *Chem. Eng. Sci.* **2014**, *111*, 657–671. [CrossRef]
14. Khan, M.S.; Ahmad, I. CFD modeling of rotary cement kilns. *Miner. Eng.* **2013**, *43–44*, 57–63. [CrossRef]
15. Zheng, K.; Liu, W.; Guo, F. Coupling heat transfer model of rotating cement kiln with accompanying evaporation-drying process. *J. Therm. Sci.* **2011**, *20*, 245–251. [CrossRef]
16. Li, C.; Feng, Y.; Hu, Z.; Luo, S. Numerical simulation of the influence factors for rotary kiln in temperature field and stress field. *J. Univ. Sci. Technol. Beijing* **2006**, *28*, 446–451.
17. Larsson, I.A.S. The Aerodynamics of an Iron Ore Pelletizing Rotary Kiln. *Fluids* **2022**, *7*, 160. [CrossRef]
18. Žiga, A.; Karač, A.; Vukojević, D. Analytical and numerical stress analysis of the rotary kiln ring. *Teh. Vjesn.* **2013**, *20*, 941–946.
19. Goshayeshi, H.R.; Poor, F.K. Modeling of Rotary Kiln in Cement Industry. *Energy Power Eng.* **2016**, *8*, 23. [CrossRef]
20. Saidur, R.; Hossain, M.S.; Islam, M.R.; Fayaz, H.; Mohammed, H.A. A review on kiln system modeling. *Renew. Sustain. Energy Rev.* **2011**, *15*, 2487–2500. [CrossRef]
21. Li, X.; Shen, Y.; Wang, S. Dynamic modeling and analysis of the large-scale rotary machine with multi-supporting. *Shock Vib.* **2011**, *18*, 53–62. [CrossRef]
22. *EN 1993-1-1*; Eurocode 3: Design of Steel Structures. European Committee for Standardization: Brussels Belgium, 1993. Available online: https://www.phd.eng.br/wp-content/uploads/2015/12/en.1993.1.1.2005.pdf (accessed on 23 October 2020).
23. Świtalski, M. The Measurement of Shell's Elastic Ovality as an Essential Element of Diagnostic of Rotary Drum's Technical State. *Diagnostyka* **2010**, *53*, 37–47.
24. Available online: https://www.zmp.com.pl/shelltester (accessed on 6 October 2020).
25. Krystowczyk, Z. Geometry Measurements of Kiln Shell in Dynamic Conditions. *Cem. Build. Mater. Rev.* **2004**, *16*, 34–37.
26. Mogil'Nyj, S.G.; Sholomitskii, A.A.; Lagutina, E.K.; Sal'Nikov, V.G. The influence of refraction in geodetic measurements of rotary kilns. In Proceedings of the 25th International Symposium on Atmospheric and Ocean Optics: Atmospheric Physics, Novosibirsk, Russia, 30 June–5 July 2019.
27. Mogilny, S.; Sholomitskii, A. Precision analysis of geometric parameters for rotating machines during cold alignment. *Procedia Eng.* **2017**, *206*, 1709–1715. [CrossRef]
28. Jia, D.; Zhang, W.; Wang, Y.; Liu, Y. A New Approach for Cylindrical Steel Structure Deformation Monitoring by Dense Point Clouds. *Remote Sens.* **2021**, *13*, 2263. [CrossRef]
29. Kovanič, L.; Blišťan, P.; Zelizňaková, V.; Palková, J.; Baulovič, J. Deformation investigation of the shell of rotary kiln using terrestrial laser scanning (TLS) measurement. *Metalurgija* **2019**, *58*, 311–314. ISSN 1334-2576.
30. Zhang, Z.; Yin, T.; Huang, X.; Zhang, F.; Zhu, Y.; Liu, W. Identification and Visualization of the Full-Ring Deformation Characteristics of a Large Stormwater Sewage and Storage Tunnel Using Terrestrial Laser Scanning Technology. *Energies* **2019**, *12*, 1304. [CrossRef]
31. Site of Open Corporation Industrial Geodesy. Available online: http://promgeo.com/services/kiln (accessed on 6 October 2020).
32. Tucci, G.; Conti, A.; Fiorini, L. Refractory Brick Lining Measurement and Monitoring in a Rotary Kiln with Terrestrial Laser Scanning. In Proceedings of the First International Workshop in Memory of Prof. Raffaele Santamaria on R3 in Geomatics: Research, Results and Review, R3GEO 2019, Naples, Italy, 10–11 October 2019; Revised Selected Papers; Springer: Berlin/Heidelberg, Germany, 2020.
33. Danila, A. The Detection of the Thermal Processes' Variations into Rotary Cement Kilns by Thermographic Imaging of the Kiln Outer Shell. In Proceedings of the 2021 25th International Conference on System Theory, Control and Computing (ICSTCC), Iasi, Romania, 20–23 October 2021; pp. 498–503. Available online: https://ieeexplore.ieee.org/abstract/document/9607315 (accessed on 10 January 2019).
34. Noshirvani, G.; Shirvani, M.; Askari-Mamani, J.; Nourzadeh, H. Estimation of coating thickness in a rotary kiln by using shell temperature and kiln modeling. *ZKG Int.* **2013**, *11*, 58–71.
35. Lamm, R.; Kirchhoff, S. Optimization of ladle refractory lining, gap and crack detection, lining surface temperature and sand filling of the ladle-taphole by means of a 3D-laser profile-measurement-system that is immersed in a hot ladle to evaluate the entire condition. In Proceedings of the UNITECR 2017, Proceedings 2017, Santiago, Chile, 26–29 September 2017. Available online: http://www.unitecr2017.mundodecongresos.com/abstracts/Paper_rbofbhfxcsxhpgipoispm.pdf (accessed on 10 January 2019).
36. Schnabel, R.; Wahl, R.; Klein, R. Efficient RANSAC for point-cloud shape detection. *Comput. Graph. Forum* **2007**, *26*, 214–226. [CrossRef]
37. CloudCompare. Vers. 2.11 Alpha. Available online: http://www.cloudcompare.org/ (accessed on 10 January 2019).
38. Kovanič, Ľ.; Blistan, P.; Urban, R.; Štroner, M.; Pukanská, K.; Bartoš, K.; Palková, J. Analytical Determination of Geometric Parameters of the Rotary Kiln by Novel Approach of TLS Point Cloud Segmentation. *Appl. Sci.* **2020**, *10*, 7652. [CrossRef]
39. Bui, T.; Beers, A.C.; van Helden, W.G.J.; Segers, A.J.H.; van Antwerpen, H.J.; van der Stappen, A.F. Integrating axis deviation and deformation control for large industrial rotary kilns. *Control Eng. Pract.* **2017**, *61*, 114–125. [CrossRef]

40. Leica RTC360. Available online: https://leica-geosystems.com/-/media/files/leicageosystems/products/datasheets/leica-rtc360-ds.ashx?la=hu-hu&hash=3C70C6ADDEB8DCA88E48A26739B4A1A6 (accessed on 10 January 2019).
41. Fischler, M. A.; Bolles, R. C. Random sample consensus: A paradigm for model fitting with applications to image analysis and automated cartography. *Commun. ACM* **1981**, *24*, 381–395. [CrossRef]